BIOCHEMISTRY
including biophysical chemistry & molecular biology

Article

pubs.acs.org/biochemistry

On the Catalytic Mechanism of Human ATP Citrate Lyase

Fan Fan,*[,†] Howard J. Williams,[‡] Joseph G. Boyer,[§] Taylor L. Graham,[†] Huizhen Zhao,[†] Ruth Lehr,[†] Hongwei Qi,[†] Benjamin Schwartz,[†] Frank M. Raushel,[‡] and Thomas D. Meek[†]

[†]Biological Reagents and Assay Development, GlaxoSmithKline, Collegeville, Pennsylvania 19426, United States

[‡]Department of Chemistry, Texas A&M University, College Station, Texas 77842, United States

[§]Department of Statistical Sciences, GlaxoSmithKline, 2301 Renaissance Boulevard, King of Prussia, Pennsylvania 19406, United States

ABSTRACT: ATP citrate lyase (ACL) catalyzes an ATP-dependent biosynthetic reaction which produces acetyl-coenzyme A and oxaloacetate from citrate and coenzyme A (CoA). Studies were performed with recombinant human ACL to ascertain the nature of the catalytic phosphorylation that initiates the ACL reaction and the identity of the active site residues involved. Inactivation of ACL by treatment with diethylpyrocarbonate suggested the catalytic role of an active site histidine (i.e., His760), which was proposed to form a phosphohistidine species during catalysis. The pH-dependence of the pre-steady-state phosphorylation of ACL with [γ-^{33}P]-ATP revealed an ionizable group with a pK_a value of ~7.5, which must be unprotonated for the catalytic phosphorylation of ACL to occur. Mutagenesis of His760 to an alanine results in inactivation of the biosynthetic reaction of ACL, in good agreement with the involvement of a catalytic histidine. The nature of the formation of the phospho-ACL was further investigated by positional isotope exchange using [γ-$^{18}O_4$]-ATP. The β,γ-bridge to nonbridge positional isotope exchange rate of [γ-$^{18}O_4$]-ATP achieved its maximal rate of 14 s^{-1} in the absence of citrate and CoA. This rate decreased to 5 s^{-1} when citrate was added, and was found to be 10 s^{-1} when both citrate and CoA were present. The rapid positional isotope exchange rates indicated the presence of one or more catalytically relevant, highly reversible phosphorylated intermediates. Steady-state measurements in the absence of citrate and CoA showed that MgADP was produced by both wild type and H760A forms of ACL, with rates at three magnitudes lower than that of k_{cat} for the full biosynthetic reaction. The ATPase activity of ACL, along with the small yet significant positional isotope exchange rate observed in H760A mutant ACL (~150 fold less than wild type), collectively suggested the presence of a second, albeit unproductive, phosphoryl transfer in ACL. Mathematical analysis and computational simulation suggested that the desorption of MgADP at a rate of ~7 s^{-1} was the rate-limiting step in the biosynthesis of AcCoA and oxaloacetate.

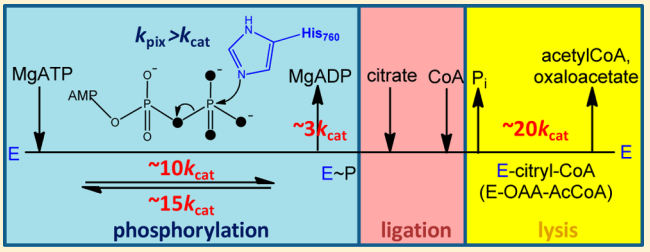

ATP citrate lyase (EC 2.3.3.8; hereafter ACL) catalyzes the MgATP-dependent biosynthesis of oxaloacetate and acetyl coenzyme A from coenzyme A (CoA) and citrate[1−7] as shown in Scheme 1. ACL plays important roles in key biosynthetic processes including gluconeogenesis,[8] lipogenesis, and cholesterolgenesis.[9] Recent studies also demonstrated that the activity of ACL can affect the acetylation of histones via mediation of glucose concentrations during cellular differentiation.[10] Purified human ACL is an apparent homotetramer comprised of ~110-kDa subunits. Mechanistic studies[5,11−13] with rat liver ACL agree with a kinetic mechanism as illustrated in Scheme 2. Briefly, MgATP binds to free ACL which catalyzes the apparent phosphorylation of an active site residue, followed by the subsequent release of MgADP. The phospho-enzyme then putatively catalyzes the formation of an enzyme-bound citryl phosphate, which is subsequently attacked by the thiol group of coenzyme A, liberating inorganic phosphate. The resulting enzyme-bound intermediate, citryl-CoA, then undergoes a retro-Claisen cleavage to yield acetyl-CoA and oxaloacetate, with oxaloacetate as the last product released from the enzyme active site. The biosynthetic reaction of ACL can therefore be divided into three partial reactions: (1) the binding of MgATP and phosphorylation of ACL, with the release of MgADP; (2) the binding and ligation of citrate to CoA, leading to the formation of citryl-CoA; and (3) the retro-Claisen reaction to form the products, acetyl-CoA and oxaloacetate.

Scheme 1

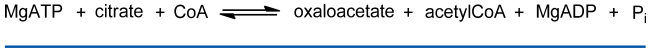

Scheme 2

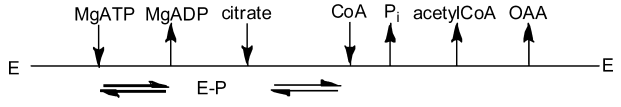

Received: May 9, 2012
Revised: May 31, 2012
Published: June 4, 2012

Since the initial kinetic characterization of mammalian ACL,[1−3,5,13] details of the chemical mechanism remain unresolved. Several key questions remain, which include (1) the validation for the involvement of a histidine residue in phosphorylation; (2) the nature of the reaction intermediates, for example, phospho-enzyme and citryl-phosphate; as well as (3) the identity of the rate-limiting step(s). The identity of the catalytically relevant phosphate acceptor in phospho-ACL has been postulated to be His760.[14−18] The first direct observation arises from the ^{31}P NMR studies by Williams et al. with rat liver ACL, for which catalytic phosphorylation was only observed under denaturing conditions (i.e., addition of 20 mM EDTA, or SDS), or with the addition of 1.5 M potassium chloride.[17] A phospho-histidinyl resonance was observed for the KCl-treated protein. The KCl-treated phospho-ACL ^{31}P NMR species was suggested to be catalytically relevant because it diminished upon the addition of citrate and CoA.[17] Kanao et al. had observed by electrophoresis the phosphorylation of His273, the corresponding catalytic histidine of the ACL from *Chlorobium limicola*, by incubating the enzyme with [γ-^{32}P]-ATP in the absence of citrate and CoA.[19] However the presumed instability of a phospho-histidyl enzyme form[20,21] presents challenges for its direct observation, since there were also documented studies with electrophoretic and radiometric methods which failed to elucidate the catalytic histidinyl phosphate.[22] In addition, the presence of regulatory phosphorylation site(s) on ACL, namely, Thr446, Ser450, and Ser454,[22−25] further complicates the identification of the appropriate residue involved in catalytic phosphoryl-transfer. Thus the identity of the catalytic phosphate acceptor remains unclear, especially for the human phospho-ACL. Independent approaches are therefore needed to provide insights. Understanding the nature of phosphoryl transfer is critical to fully characterize the catalytic mechanism of human ACL. Since the rate-determining step(s) of ACL are also unknown, it is important to address this question so as to enable the most practical means of modulating the action of ACL.

Here we present a detailed kinetic characterization using chemical modification, rapid-quench kinetics, positional isotope exchange, as well as mathematical modeling and kinetic simulation to achieve an in-depth understanding of how ACL catalyzes the biosynthesis of acetyl-CoA and oxaloacetate. The studies were carried out on both wild type ACL, as well as a His760 mutant form of the enzyme, to probe the catalytic role of this conserved residue.

EXPERIMENTAL PROCEDURES

Materials. *pfu* DNA polymerase was from Agilent Technologies. T4 DNA ligase and the restriction enzymes *NdeI* and *Eco*RI were purchased from New England Biolabs. The oligonucleotide primers were synthesized by Integrated DNA Technologies. The pFastBac plasmid harboring wild type ACL was obtained in-house (GlaxoSmithKline). The Bac-to-Bac Baculovirus Expression system was from Invitrogen Life Technologies. HyClone SFX-Insect Cell Culture medium was purchased from Thermo Scientific. All chromatographic materials were from Amersham Pharmacia. Phosphate Sensor (Life Technology) was purchased from Invitrogen. Sodium citrate was from Calbiochem. ADP Glo was purchased from Promega. Human malate dehydrogenase (type 2) was received from the Structural Genomic Consortium (The University of Oxford, United Kingdom), and was purified following the protocol as described by the SGC.[26] [γ-^{33}P]-ATP (3000 C_i/mmol) was purchased from PerkinElmer Life Sciences. [γ-$^{18}O_4$]-ATP was prepared by WuXi AppTec (Shanghai) Co. LTD, as described previously.[27] The 96-well MultiScreen$_{HTS}$-HA plates were from Millipore. All other chemicals were purchased from Sigma or Aldrich of the highest available purity.

Site-Directed Mutagenesis. An H760A mutation was introduced using the Agilent Technologies' QuickChange II XL Site-Directed Mutagenesis kit in accordance with the manufacturer's instructions. The pFastBac plasmid harboring wild type ACL was used as a template. The forward primer with nucleotide sequence of 5′-GTTCTCCTCTGAG-GTCCAGTTTGGCgcTGCTGGAGCTTGTGCCAACCAG-GCTTC-3′; and reverse primer with nucleotide sequence of 5′-GAAGCCTGGTTGGCACAAGCTCCAGCAgcGCC-AAACTGGACCTCAGAGGAGAAC-3′ were used to introduce the desired alanine mutation. The construct was confirmed by standard in-house DNA sequencing.

Expression and Purification of the H760A Mutant Form of ACL. A mutant form of ACL, H760A was expressed using the Bac-to-Bac system (Life Technology). One liter of sf9 cells was infected with Baculovirus stocks at a multiplicity of infection (MOI) of 0.5, when the cell density reached to 1.8×10^6 cells/mL. The cells were grown at 27 °C and were harvested at 50 h postinfection followed by centrifugation at 3800*g* for 20 min at 4 °C. Cells were then lysed by sonication. The mutant enzyme was purified to apparent homogeneity using the same protocol as for the wild type ACL.[28] The purified protein was evaluated by SDS−PAGE according to the method of Laemmli.[29] The concentration of enzyme was determined using the Bio-Rad protein assay kit for which bovine serum albumin was used as a standard.[30]

Kinetic Assays. Initial velocities of the ACL reaction were carried out in 10 μL of 50 mM Tris, 10 mM $MgCl_2$, and 2 mM DTT (pH 8), at room temperature. Enzymatic products were quantified by three different assay formats. The inorganic phosphate formed was measured by the Phosphate Sensor reagent, for which the fluorescence intensity increase was measured continuously at 430/450 nM (ex/em) as described by following the manufacturer's instruction. Product ADP was measured using the ADP Glo Kinase assay kit. Aliquots (5 μL) were withdrawn at 5−10 min intervals over a period of 60 min, from 50 μL reaction mixtures, and added to 5 μL ADP Glo (Reagent 1). After a 1 h incubation, 10 μL of ADP Glo reagent 2 was added, as instructed by the manufacturer's protocol. The generated luciferase/luciferin signal was measured using an EnVison fluorimeter (2104 Multilabel Reader, with luminescence aperture). The product oxaloacetate was quantified using a coupled-enzyme assay in the above buffer conditions. The 50 μL reaction mixture contained additional malate dehydrogenase (10 units) and 300 μM NADH.[4] The consumption of NADH was followed spectrophotometrically at 340 nM. Typically, the reaction mixture contained 2−3 nM of wild type ACL or ∼500−700 nM of mutant ACL.

Chemical Modification by Diethylpyrocarbonate. ACL (1.42 μM) was preincubated at room temperature in reaction mixtures containing 68 μM diethylpyrocarbonate (DEPC), 50 mM MOPS (pH 7.5), 10 mM $MgCl_2$, 2 mM DTT, with and without 0.5 mM ATP. Aliquots of 20 μL were withdrawn at 10−90 min intervals and were desalted by application to Zeba spin desalting columns (7K MWCO, Thermo Scientific) that were pre-equlibrated with the incubation buffer. The desalting process was carried out by following the manufacturer's instruction. The resulting effluents were assayed for residual

dx.doi.org/10.1021/bi300611s | *Biochemistry* 2012, 51, 5198−5211

ACL activity using the Phosphate Sensor assay at 1 mM concentrations of all three substrates. Also the desalted samples were evaluated spectrophotometrically (200−400 nm). The samples were then treated with 10 mM freshly prepared hydroxylamine solution (prepared in 50 mM MOPS pH 7.0). After desalting by use of Zeba spin columns, residual enzymatic activity was subsequently measured using the Phosphate Sensor assay as described above.

Pre-Steady-State Kinetics. Single-turnover experiments were performed at room temperature using a KinTek rapid quench apparatus (model RQF-3). The transient rates of the first half-reaction (enzyme phosphorylation) were determined by rapidly mixing equal, ∼20 μL volumes of two solutions, one containing ACL with 2 mM DTT in 50 mM buffer (Tris or BisTris), and the other solution containing [γ-^{33}P]-ATP (20 μCi/μmol) and 10 mM $MgCl_2$ in the same buffer. Three types of rapid kinetic experiments were carried out. In the first set of experiments, 3 mM [γ-^{33}P]-ATP was reacted with 1.47 μM ACL (5.86 μM of active sites) in 50 mM Tris (pH 8), with and without 1 mM citrate or 1 mM citrate and CoA. The second set of experiments was carried out using 5.86 μM ACL (active site concentration) also containing 1 mM citrate and CoA. The ACL solution was mixed with varying concentrations of [γ-^{33}P]-ATP solutions, ranging from 0.03 to 3 mM. The third set of experiments examined the pH-dependence of the phosphorylation of ACL in the binary reaction of enzyme and MgATP, at 5.46 μM ACL (active site concentration, prior to mixing). The MgATP solution contained 2 mM [γ-^{33}P]-ATP and 10 mM $MgCl_2$. Both solutions were prepared in 50 mM BisTris, at pH values ranging from 6.5 to 9.5. For all three types of experiments, control samples contained enzyme that was pre-inactivated with 0.2 M EDTA. The reaction mixtures containing ACL (with or without citrate or citrate and CoA) and ATP were "aged" for reaction times of 0.005−10 s, and then quenched with ∼106 μL of 200 mM EDTA; 25-uL reaction mixtures were loaded onto a 96-well MultiScreen$_{HTS}$-HA plate, which was pre-equilibrated with 50 mM reaction buffer, with addition of 2 mM ATP and 10 mM phosphate. A vacuum was then applied to the plate, followed by washing the plate with equilibration buffer. After repeating the vacuum-washing cycle five times, plates were dried in a 40 °C oven for 20 min. Subsequently, 60 μL of micro-scintillation fluid (MicroScint 20, Perkin-Elmer) was added into each well, and residual radioactivity in samples was quantified using a Topcount scintillation counter (Perkin-Elmer, NXT, HTS).

Positional Isotope Exchange. The positional isotope exchange of [γ-$^{18}O_4$]-ATP was determined by the time-dependent decrease and increase, respectively, of the [γ-$^{18}O_4$]-ATP and [γ-^{16}O, $^{18}O_3$]-ATP species as ascertained by ^{31}P NMR. The reaction mixtures contained 3 mM [γ-$^{18}O_4$]-ATP, 10 mM $MgCl_2$, 2.0 mM DTT, 50 mM HEPES (pH 8), 21 nM wild type or 1.28 μM H760A mutant form of ACL. Reactions were performed with or without citrate or citrate and CoA (both at 1.5 mM concentrations in the reaction mixtures). The total reaction mixtures (2.6 mL) were incubated at room temperature for 2 h. Aliquots with volumes of 416 μL were withdrawn at 5−120 min intervals, and each aliquot was quenched by adding 104 μL of 0.5 M EDTA, followed by boiling of the samples for 2 min. After centrifugation at 20000g for 10 min to remove precipitated protein, 400 uL of the resulting supernatant was withdrawn, to which 100 μL of D_2O was added. ^{31}P NMR spectra were acquired using a Bruker Avance III-400 NMR spectrometer operating at a frequency of 162 MHz. Acquisition parameters were 4900-Hz sweep width, 1.7 s acquisition time, and a 1.0 s delay between pulses.

Mathematical Modeling and Kinetic Simulation. The estimation of kinetic rate constants was conducted using the Levenberg−Marquardt algorithm as implemented in the NLIN procedure of the SAS statistical programming language (SAS Institute InC, Verson 9.2). Simulation was carried out using KinTek Global Kinetic Explorer (Version 3.0, KinTek Corp, Austin TX) for the rapid kinetic data, following the user's manuals.

Data Analysis. Residual ACL activity following preincubation with DEPC was fitted by eq 1, in which A_o is the activity at time zero, A_t is the activity at time t, t is time in minutes, and k_{obs} is the apparent rate constant of inactivation (min^{-1}). Pre-steady-state kinetic data were fitted to eq 2, in which Y is the isolated product [^{33}P]-ACL (μM), β is the burst amplitude (μM), t is time in sec, and λ is the apparent transient rate constant (s^{-1}). For a two-step mechanism, the dependence of a single exponential rate constant (λ), and the burst amplitude (β), as a function of the substrate concentration is given by eqs 3 and 4, respectively, for which λ_{max} and β/E_{tmax}, are maximal values of each parameter, K_{d1}, K_{d2}, and K_{d3} are factors composed of the dissociation constant of the variable substrate (K_{d1}) and individual rate constants (K_{d2}, K_{d3}).

The pH dependence of pre-steady-state kinetic parameters were determined by fitting initial rate data to eq 5, which describes a curve with a slope of 1 at low pH and a plateau at high pH. The data were also fitted to eq 6, which describes a bell-shaped curve with a slope of 1 at low pH, and a slope of −1 at high pH. The pK_a value describes the pH value at which 50% of the ionizable group (catalytic acid) is protonated for catalysis; the pK_b value describes the pH value at which 50% of the ionizable group (catalytic base) is unprotonated for catalysis.

The rate constant for the progression of positional isotopic exchange to equilibrium within the γ-P species of ATP was obtained by fitting the data to eq 7. This equation accounts for the fraction of [^{18}O]-labeling in [γ-$^{18}O_4$]-ATP that will undergo positional isotope exchange.[31] The number of species (n) that will show a reduction in the fraction of [γ-$^{18}O_4$]-P is 2, and the number of species (m) that will not result in a decrease in the fraction of [γ-$^{18}O_4$]-P is 1. Y_4 is the amount of the [γ-$^{18}O_4$]-P species at time t, Y_t is the sum of all isotopic species in the γ-P species, and all other values are as previously defined.

$$\log Y = A_t e^{(-k_{obs}t)} + A_0 \quad (1)$$

$$Y = \beta(1 - e^{-\lambda t}) \quad (2)$$

$$\lambda = \frac{[\lambda_{max}S + K_{d2}]}{K_{d1} + S} \quad (3)$$

$$\frac{\beta}{E_t} = \frac{\frac{\beta_{max}}{E_t}S}{K_{d3} + S} \quad (4)$$

$$\log Y = \log\left(\frac{C}{1 + \frac{10^{-pH}}{10^{-pKa}}}\right) \quad (5)$$

dx.doi.org/10.1021/bi300611s | Biochemistry 2012, 51, 5198−5211

$$\log Y = \log\left(\frac{C}{1 + \frac{10^{-pKa2}}{10^{-pH}} + \frac{10^{-pH}}{10^{-pKa1}}}\right) \quad (6)$$

$$\frac{Y_4}{Y_t} = Z^4\left(1 + \frac{ne^{-v_{ex}t}}{n+m} - \frac{n}{n+m}\right) \quad (7)$$

RESULTS

Chemical Modification by DEPC. To obtain understanding regarding the active site residue(s) of ACL, enzyme inactivation of ACL arising from covalent modification by DEPC was evaluated both by measurement of residual enzymatic activity (Phosphate Sensor assay) after pretreatment and by measurement of the spectrophotometric properties of the modified enzyme. DEPC reacts differentially with histidine, cysteine, lysine, and tyrosine residues in proteins to form N-carboethoxy adducts.[32,33] With histidine residues, DEPC reacts with the N^3 nitrogen of the imidazole substituent.[32,33] The resulting N-carboethoxy group has a signature absorbance peak at 240 nm. In the current study with ACL, the peak at 240 nm was not observed. This is probably due to dilution of the low concentration of ACL (~1 μM) following desalting of the treated ACL which would contribute only a ~0.003 absorbance unit increase.[34] The remaining activity of the desalted, DEPC-treated ACL as a function of time fitted best to a single exponential model, suggesting that a single active site group was being modified by DEPC. Interestingly the addition of 0.5 mM ATP in the preincubation reaction mixture provided complete protection of ACL activity from inactivation by DEPC (Figure 1). This suggested that the DEPC-modified residue is involved

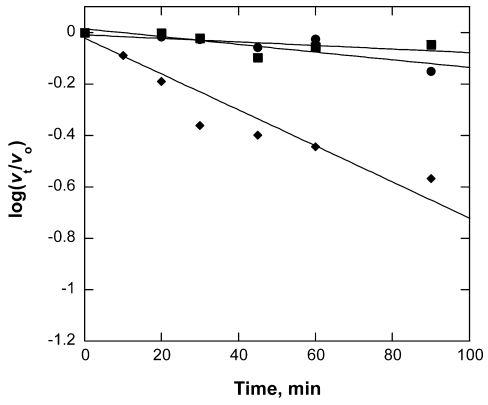

Figure 1. DEPC inactivation of ACL. The logarithm of the fractional percent of residual activity was plotted as a function of time. The three lines shown are control (no DEPC added, ●), 67.9 μM DEPC added (♦), and 67.9 μM DEPC and 0.5 mM ATP added (■). The values are averages of duplicate determinations. The data were fitted to eq 1, and the rate constant was calculated to be $k = 0.0003$ min^{-1} from the curve represented by (♦).

in the observed phosphoryl transfer reaction of the binary ACL−MgATP complex. Although the expected spectrophotometric species (at 240 nm) was not observed from our studies, the observation that the reactivation of the enzyme activity (~45% of the initial activity) could be achieved by adding freshly prepared hydroxylamine (data not shown). This is indicative of the reversal of histidine modification that arises from the putative deacylation of the N-carboethoxy-histidinyl adducts, which is expected to be chemically more facile than deacylation of lysyl or cysteinyl adducts.

Steady-State Measurements of ATPase and Biosynethic Reactions. Steady-state kinetics of both the wild type and H760A mutant of ACL was performed using assays that detected three different reaction products: phosphate, MgADP, and oxaloacetate, and under two sets of reaction conditions: a biosynthetic reaction in which MgATP, citrate, and CoA were present with enzyme and an ATPase reaction in which only MgATP and enzyme were present. Results are summarized in Table 1. For the biosynthetic reaction of wild type ACL, an average turnover number of 2.4 ± 0.9 s^{-1} and apparent Michaelis constants are as shown in Table 1, and average values of $k_{cat}/K_{MgATP} = 0.019 \pm 0.007$ μM^{-1} s^{-1}, $k_{cat}/K_{citrate} = 0.23 \pm 0.07$ μM^{-1} s^{-1}, and $k_{cat}/K_{CoA} = 0.24 \pm 0.11$ μM^{-1} s^{-1} were obtained. For the ATPase reaction, the rates of production of both product MgADP ($k_{cat} = 0.008 \pm 0.001$ s^{-1}) and phosphate were extremely low, indicating that either MgATP is very slowly hydrolyzed by ACL, or that phosphorylation of ACL occurs to form phospho-ACL-MgADP from which MgADP only slowly desorbs. Alternatively, the measured rates of production of phosphate and MgADP could be nonenzymatic. The low activity, with a signal to background ratio equal to 2−3, makes quantitative determination of ATPase reaction extremely challenging.

Mutagenesis, Expression, Purification, and Steady-State Kinetics of H760A ACL. Inactivation of human ACL by preincubation with DEPC suggested that the highly conserved residue, His760, plays a role in phosphoryl transfer from ATP. Accordingly, we prepared mutant forms of ACL at this residue to further characterize the mechanistic role of His760, as well as to provide additional mechanistic insights into ACL catalysis. The H760A mutant of ACL was obtained by expression in Sf9 cells, and the H760A ACL was purified to apparent homogeneity. The final yield of purified human H760A ACL was ~35 mg from 1 L of cell culture, which eluted as an apparent tetramer upon gel filtration chromatography on a column of Superose 12, similar to that of wild type ACL. The relative subunit molecular mass of purified H760A ACL was determined by SDS−PAGE to be ~110 kDa, as was observed for wild type ACL. Nucleotide sequencing confirmed the presence of an alanyl residue in position 760.

H760A ACL was assayed for phosphate formation using the phosphate sensor, MgADP generation using ADP Glo, and for oxaloacetate generation using the malate dehydrogenase coupled-enzyme assay. The H760A mutant exhibited the ability to generate inorganic phosphate and MgADP, albeit at very low rates of catalysis, as observed by using the phosphate sensor and ADP-Glo assays, respectively, in reaction mixtures containing mutant enzyme and MgATP (with or without the addition of citrate and CoA). This suggested that H760A ACL promotes an ATPase reaction which may involve the phosphorylation of an enzymatic residue. The turnover number of H760A ACL is similar to that of wild type in the absence of citrate and CoA, yet significantly less than that of wild type ACL in the presence of both citrate and CoA. Quantification of the full biosynthetic reaction of H760A ACL using the malate dehydrogenase coupled assay, showed no production of oxaloacetate. Since this continuous, spectrophotometric assay is less sensitive compared to either the fluorescence or luciferase-based assays, an end-point MDH assay was also carried out. The mixture, containing 2 μM H760A ACL, 1 mM MgATP, 5 mM $MgCl_2$, citrate, and CoA, was incubated at

dx.doi.org/10.1021/bi300611s | Biochemistry 2012, 51, 5198−5211

Table 1. Steady-State Kinetics Results for Wild Type and H760A ACL[a]

Full Biosynthetic Reaction[b]					
			product measured		
ACL	parameters	fixed substrates[c]	phosphate	MgADP	oxaloacetate[d]
WT	k_{cat}, s^{-1}	citrate, CoA	1.6 ± 0.1	2.2 ± 0.1	3.4 ± 0.7
	K_{MgATP}, μM	citrate, CoA	149 ± 40[e]	144 ± 60	90 ± 31
	$K_{citrate}$, μM	MgATP, CoA	7 ± 1	4 ± 1	20 ± 6
	K_{CoA}, μM	MgATP, citrate	12 ± 3	10 ± 3	8 ± 3
H760A	k_{cat}, s^{-1}	citrate, CoA	0.006 ± 0.0002	0.006 ± 0.001	N.A.[f]
	K_{MgATP}, μM	citrate, CoA	74 ± 18	110 ± 40	N.A.[f]
	$K_{citrate}$, μM	MgATP, CoA	4 ± 1	N.D.	N.A.[f]
	K_{CoA}, μM	MgATP, citrate	8 ± 2	N.D.	N.A.[f]
ATPase Reaction[g]					
			products measured		
ACL	parameters	fixed substrates	phosphate[h]	MgADP	oxaloacetate[f]
WT	k_{cat}, s^{-1}	N.A.	0.0001 ± 0.00003	0.008 ± 0.001	N.A.
	K'_{MgATP}, μM	N.A.	150 ± 60	50 ± 28	N.A.
H760A	k_{cat}, s^{-1}	N.A.	0.0006 ± 0.0002	0.007 ± 0.002	N.A.
	K_{MgATP}, μM	N.A.	380 ± 130	109 ± 36	N.A.

[a]Experiments performed as described in Experimental Procedures. [b]The data are from the experiments with addition of all three substrates. [c]Fixed concentrations are at saturating levels, that is, at 1 mM citrate and CoA, and 1.5 mM MgATP. [d]The results from MDH assay are slightly different comparing to phosphate sensor and ADP-Glo assays. However, within experimental errors, the values are considered to be similar between assay platforms. [e]The values of K_m were obtained by averaging five different experiments (data not shown). [f]No activity can be detected with MDH absorbance assay. [g]The data are from the experiments in the absence of citrate and CoA. [h]The values from the phosphate sensor assay in the absence of citrate and CoA could not be used to draw quantitative conclusions due to the low reactivity. Under this condition, the signal increase from phosphate release does not separate well from the noise level (≤3 fold).

room temperature for 60 min. 300 μM NADH, and 20 units of malate dehydrogenase were subsequently added into the reaction mixture. However, no decrease of NADH was observed, indicating that mutant ACL was incompetent to catalyze the full biosynthetic reaction. The measurements of ADP and phosphate product in the absence of citrate and CoA further support the notion of unproductive phosphorylation in ACL. The results are summarized in Table 1.

Pre-Steady-State Kinetics. The rate of phospho-enzyme formation in the first partial reaction (binary reaction) was evaluated by using rapid-quench flow techniques and [γ-^{33}P]-ATP. For wild type enzyme, the rapid kinetics studies were performed with three sets of reaction mixtures: (1) binary reaction: ACL mixed with 1.5 mM [γ-^{33}P]-ATP and 5 mM $MgCl_2$; (2) ternary reaction: ACL mixed with 1.5 mM [γ-^{33}P]-ATP, 5 mM $MgCl_2$, and 0.5 mM citrate; (3) quaternary (biosynthetic) reaction: ACL mixed with 1.5 mM [γ-^{33}P]-ATP, 5 mM $MgCl_2$, 0.5 mM citrate, and 0.5 mM CoA. The time courses for the formation of [γ-^{33}P]-ACL were fitted to eq 2 to obtain the transient kinetic rate constants and burst amplitudes for the formation of isolable phospho-ACL species. The concentrations of isolated [^{33}P]-ACL species were plotted as a function of time (Figure 2). The time courses obtained for all three reaction conditions displayed rapid transient rates (λ) at <50 ms, that then reached apparent steady-state levels (burst amplitudes, β), which remained unchanged for the remainder of the 2 s reaction time courses. Data are summarized in Table 2. Under conditions of both the ATPase reaction (binary reaction; enzyme + MgATP) and ternary reaction (enzyme + MgATP + citrate), isolated ACL is apparently phosphorylated stoichiometrically by [γ-^{33}P]-MgATP in rapid transient phases. For the binary and ternary reactions, these data suggested that ACL catalyzes the formation of one or more stable phospho-enzyme species that do not progress to form free enzyme. It is likely that the transitory E-[^{33}P]-MgATP and E-[^{33}P]-MgATP-citrate complexes proceed to form quantitative amounts of the

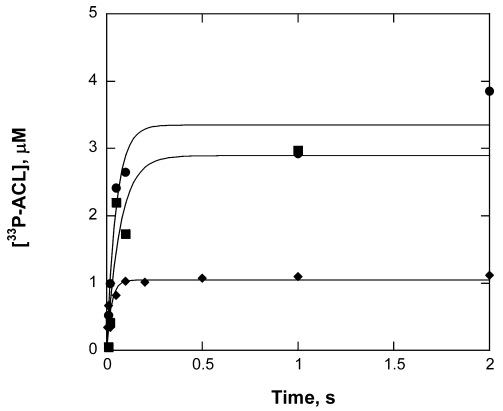

Figure 2. Rapid kinetics for wild type ACL (2.93 μM, by active site) using [γ-^{33}P]-ATP as substrate, in the absence (●), or the presence of 0.5 mM citrate (■), or the presence of 0.5 mM citrate and 0.5 mM CoA (♦). The curves were fitted to eq 2. Experiments were carried out under conditions described in Experimental Procedures.

Table 2. Summary of Pre-Steady-State Kinetic Data for Wild-Type ACL[a,b]

reaction mixture	λ, s^{-1}	β, μM	β/E_t[c], %
E + MgATP	20 ± 5	3.3 ± 0.3	110 ± 10
E + MgATP + citrate	14 ± 7	2.9 ± 0.5	98 ± 50
E + MgATP + citrate + CoA	41 ± 12	1.0 ± 0.1	34 ± 10

[a]Reaction mixtures contained 1.5 mM [γ-^{33}P]-ATP and 2.95 μM ACL (by active site), as described in Experimental Procedures. [b]Data were obtained by fitting to eq 2. [c]Stoichiometry was determined using the ratio of burst magnitude (β) to the concentration of active sites, based on the assumption that all four active sites act in similar fashion.

dx.doi.org/10.1021/bi300611s | Biochemistry 2012, 51, 5198−5211

corresponding isolable and essentially irreversible, [^{33}P]-phospho-E-MgADP and [^{33}P]-phospho-E-MgADP-citrate complexes. These transitory complexes do not attain true steady-state levels. Rather after several reversible formations of transitory complexes, transitory E-[^{33}P]-MgATP and E-[^{33}P]-MgATP-citrate have all been converted to the stable [^{33}P]-phospho-E-MgADP and [^{33}P]-phospho-E-MgADP-citrate species. These results are in agreement with those found for the rat liver citrate lyase wherein [^{32}P]-labeled ACL could be chromatographically isolated.[5] The exceedingly low steady-state rate observed for the binary reaction indicated that the quantitative formation of [^{33}P]-ACL likely reflects two enzyme forms, phospho-ACL-MgADP and phospho-ACL. In the ternary reaction, quantitative formation of [^{33}P]-ACL represents the same phospho-ACL-MgADP and phospho-ACL enzyme forms, along with phospho-ACL-citrate, but without the subsequent formation of ACL-citryl-phosphate, inasmuch as this latter species would not remain enzyme-bound under the isolation conditions.

As shown in Figure 3A, pre-steady-state kinetics of the biosynthetic (quaternary) reaction also displayed a rapid transient rate which reached a burst amplitude equivalent to 34% of the active site concentration of ACL, followed by a time course with no apparent rate. The relative reduction in the burst amplitude of the quaternary reaction indicated that under biosynthetic conditions, stable, phospho-ACL species constitute one-third of all enzyme species at steady-state, as would be expected for conditions in which phospho-enzyme forms proceed to the formation of all enzymatic species and products in a full turnover.

Similarly, the biosynthetic reaction was evaluated at different concentrations of MgATP with concentrations of citrate and CoA (each at 0.5 mM) which greatly exceeded the values of their Michaelis constants (Figure 3A). Replotting of the observed burst transient rate constant λ as a function of MgATP concentration using eq 3 yielded a maximal burst rate of $\lambda_{max} = 60 \pm 9\ s^{-1}$, and values of $K_{d1} = 500 \pm 200\ \mu M$ and $K_{d2} = 600 \pm 1600\ \mu M$ (Figure 3B). Replotting of the ratio of the apparent burst amplitude to enzyme active sites (β/E_t) by use of eq 4 yielded a maximal value of $\beta/E_{tmax} = 0.39 \pm 0.02$ and $K_{d3} = 120 \pm 23\ \mu M$ for the biosynthetic reaction conditions, indicating that ~40% of the isolated wild type ACL was stably phosphorylated when all three substrates were presented and saturating (Figure 3C).

Rapid kinetic measurements were also performed with the H760A mutant form of ACL with 1 mM [γ-^{33}P]-ATP in the presence and absence of 0.5 mM citrate and 0.5 mM CoA. However, no phosphorylated ACL H760A was isolable after 10 min postmixing reaction times. From this it is clear that if phosphorylated forms of ACL H760A are produced in this study, they are not stable to isolation.

The pH-dependence of the pre-steady-state formation of [^{33}P]-ACL was determined using 2.73 μM wild type ACL and 1 mM [γ-^{33}P]-ATP (in 50 mM BisTris, pH 6.5−9.5, as described in Experimental Procedures), in the absence of citrate and CoA, to directly probe aspects of the chemical mechanism during the phosphorylation event. Pre-steady-state kinetics were measured at pH = 6.5−9.5, and summarized in Table 3. The transient burst rate constant, λ, as a function of pH, is shown in Figure 4A, which shows that the λ values increased with increasing pH, and reached a plateau above pH 8. Fitting of this plot to eq 5 indicated that phosphorylation of ACL proceeds when an enzymatic residue with $pK_a = 7.5 \pm 0.3$ is unprotonated. Figure 4B shows the burst amplitude (β) as a function of pH, yielding a pK_a value of 6.6 ± 0.1 by fitting the data to eq 5.

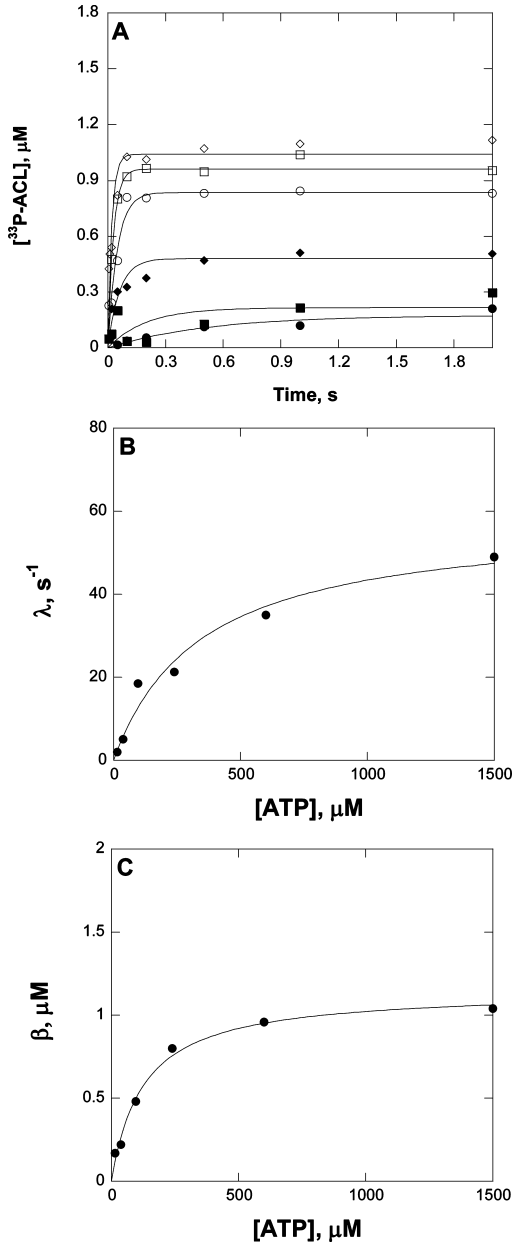

Figure 3. Rapid kinetic studies for wild type ACL (2.93 μM, by active site) in the presence of 0.5 mM citrate and CoA. (A) Traces of time courses, using variable concentrations of [γ-^{33}P]-ATP at 15.36 (●), 38.4 (■), 96 (♦), 240 (○), 600 (□), and 1500 (◊) μM. The pre-steady-state transient rate (λ) was obtained by fitting the data to eq 2. (B) Replot of the pre-steady-state transient rate (λ) versus the concentration of MgATP. (C) Replot of the burst amplitude (β) versus the concentration of MgATP where [ACL] = 2.93 μM so that $\beta/E_t = 0.34$ at 1.5 mM MgATP). The curves drawn through the data in (B) and (C) were obtained by respective fittings of the data to eqs 3 and 4. Experiments were carried out under conditions described in Experimental Procedures.

Positional Isotope Exchange. The formation of the putative phospho-ACL intermediate was explored by positional isotope exchange[31] using [γ-$^{18}O_4$]-ATP. When 3 mM [γ-$^{18}O_4$]-ATP and 10 mM $MgCl_2$ were incubated with 21 nM ACL in the absence of citrate and CoA, scrambling of ^{18}O from the β,γ-bridge to β-nonbridge positions was observed (Scheme 3), as

dx.doi.org/10.1021/bi300611s | Biochemistry 2012, 51, 5198−5211

Table 3. pH-Dependence of ACL Pre-Steady-State Kinetic Parameters[a,b]

pH	λ, s^{-1}	β, μM
6.5	4.6 ± 3.0	0.7 ± 0.1
6.8	25 ± 10	1.1 ± 0.2
7.0	62 ± 22	1.1 ± 0.1
7.5	15 ± 8	1.2 ± 0.1
8.0	78 ± 20	1.8 ± 0.2
8.5	140 ± 34	1.8 ± 0.4
9.0	64 ± 31	1.6 ± 0.1
9.5	123 ± 55	1.2 ± 0.1

[a]Experiments were carried out with 1 mM [γ-^{33}P]-ATP, as described in Experimental Procedures. [b]Data were obtained by fitting single turnover time course to eq 2.

measured by the commensurate decrease of the [γ-$^{18}O_4$] species and increase in the [γ-$^{16}O^{18}O_3$]-ATP species in the ^{31}P NMR spectrum of [γ-$^{18}O_4$]-ATP (Figure 5). These results demonstrated that reversible phosphoryl-transfer from [γ-$^{18}O_4$]-ATP to ACL readily occurred in the binary reaction. The rates of positional isotope exchange were monitored by measuring the fractional decrease of the [γ-$^{18}O_4$]-P species of the labeled ATP as a function of time. Initially, the proportion of the [γ-$^{18}O_4$]-ATP and [γ-$^{16}O^{18}O_3$]-ATP species at time zero are 76% and 24%, respectively, because each of the four oxygen atoms bonded to phosphorus is ~95% ^{18}O. The percentage of $^{18}O_4$ species decreased to 65%, 55%, 39%, 37%, and 34% in total NMR signal for the γ-resonances after 15, 30, 60, 90, and 120 min, respectively, as shown in Figure 7.

The limiting rate of positional isotope exchange for [γ-$^{18}O_4$]-ATP with wild type ACL (binary reaction; enzyme and [γ-$^{18}O_4$]-ATP only) was obtained by fitting the data in Figure 6A to eq 7, yielding a rate constant for the approach to equilibrium of 0.0237 ± 0.0013 min^{-1}, which results in a turnover number for the PIX reaction[34] of $k_{pix\text{-}bi}$ = 14 s^{-1}. In the presence of citrate or citrate and CoA, PIX was also observed albeit at slower rates than that found with [γ-$^{18}O_4$]-ATP alone, as shown in Figure 6A. The PIX data are summarized in Table 4. The maximum value of $k_{pix\text{-}bi}$ = 14 s^{-1} was observed under conditions with wild type ACL and 3 mM [γ-$^{18}O_4$]-ATP. From Figure 6A, it is evident that positional isotope exchange has nearly reached equilibrium; that is, the scrambling of ^{18}O from the bridge to nonbridge position of [γ-$^{18}O_4$]-ATP was nearly complete. Accordingly, in the absence of citrate and CoA, the transfer of the γ-phosphate of MgATP to ACL is highly reversible and apparently much more rapid than the release of MgADP from ACL. Accordingly, the stoichiometrically phospho-ACL species observed in the pre-steady-state kinetics of the binary reaction, which does not generate "catalytic" amounts of MgADP, is most likely to be phospho-ACL-MgADP and not phospho-ACL, since only the former species is competent to catalyze resynthesis of MgATP. This finding suggests that the kinetic mechanism depicted in Scheme 2 is not operative in the ATPase reaction as one would expect MgADP to be facile in the absence of citrate and CoA.

This rapid phosphoryl-transfer decreased in the presence of citrate ($k_{pix\text{-}ter}$ = 5 s^{-1}), indicating that the binding of citrate to phospho-ACL, which occurs after desorption of MgADP, traps phospho-ACL in a form from which further PIX of E-phospho-MgADP is abrogated. With the addition of CoA to a reaction mixture containing wild type ACL, [γ-$^{18}O_4$]-ATP, and citrate, the value of k_{pix} = 10 s^{-1} was greater than that observed with [γ-$^{18}O_4$]-ATP and citrate, demonstrating that under conditions of the full biosynthetic reaction, PIX occurs at a more robust rate. This augmentation is likely due to the fact that ACL substrates are fully turned-over under biosynthetic reaction conditions, as opposed to remaining "arrested" in a ternary phospho-ACL-citrate or ACL-citryl-P complex in a partial reaction. This is also reflected in the value of the maximal burst amplitude (β/E_{tmax} = 0.39) in that the phospho-ACL species comprises only 40% of all enzyme forms under steady-state conditions of the biosynthetic reaction.

With the H760A mutant enzyme, PIX studies were performed to further the understanding of His760 in its role for the phosphorylation in ACL catalysis. As shown in Figure 6B, the mutant form of ACL catalyzes a slow, but measurable, positional isotope exchange of [γ-$^{18}O_4$]-ATP, in the absence and presence of citrate and/or CoA. The rate constant for PIX of H760A mutant with a different combination of substrates are ~70−160 fold lower in comparison to corresponding conditions of wild type ACL (Table 4).

Data Fitting and Kinetic Simulation of the Biosynthetic Reaction of ACL. A computational approach was used to gain a comprehensive analysis of the observed steady-state, pre-steady-state, and positional isotope exchange data to help identify candidate values for the individual rate constants and to ascertain the rate-limiting step(s) of the biosynthetic reaction of

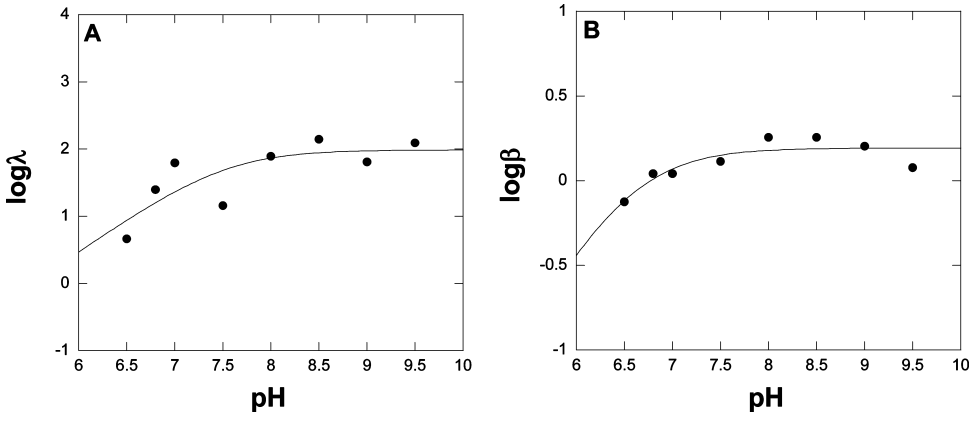

Figure 4. The pH-dependence of pre-steady-state kinetics of the phosphorylation of ACL under binary reaction conditions, for (A) the transient rate of phosphorylation of ACL (λ, s^{-1}), and (B) the burst amplitude of formation of phospho-ACL (β, μM). The curves were fitted to eq 5, for which the limiting values were determined for log λ and log β as 1.95 and 0.23, respectively.

dx.doi.org/10.1021/bi300611s | Biochemistry 2012, 51, 5198−5211

Scheme 3

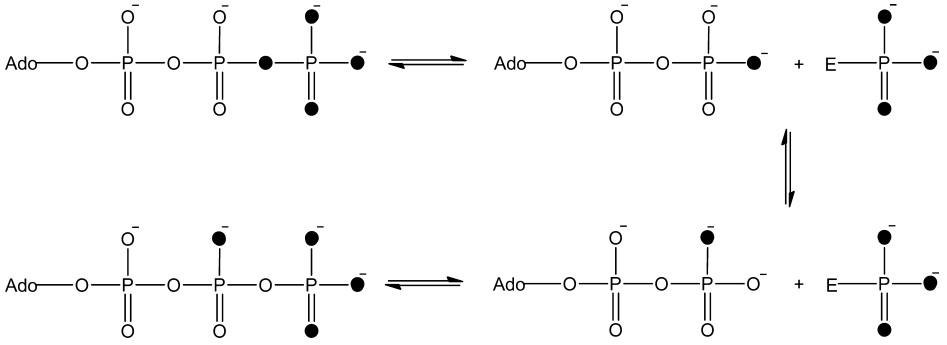

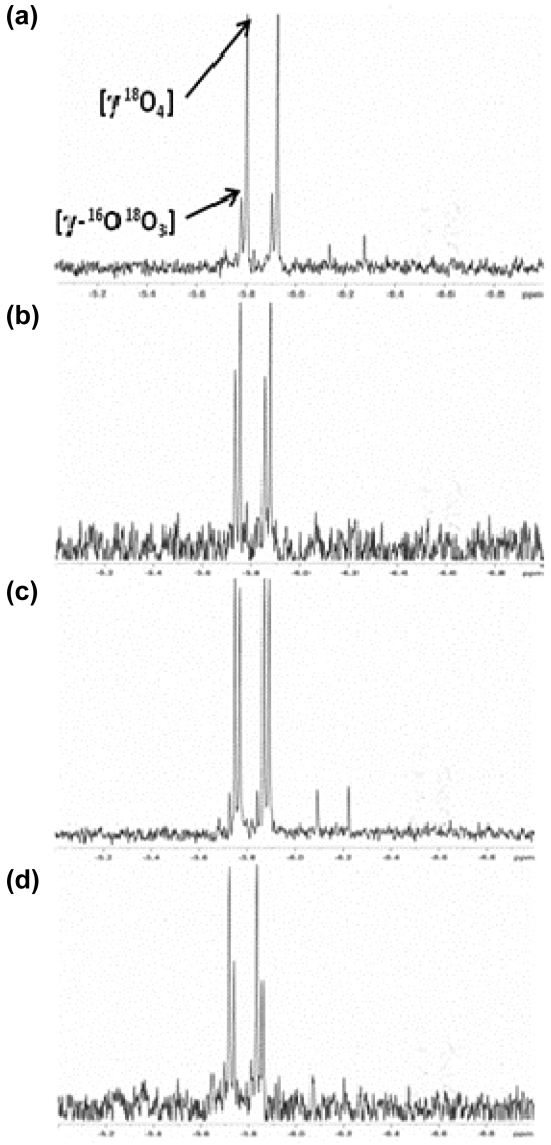

Figure 5. Positional isotope exchange of [γ-$^{18}O_4$]-ATP as catalyzed by ACL. ^{31}P NMR spectra of [γ-$^{18}O_4$]-ATP at various incubation times for wild type ACL, for changes in the isotopic composition of the γ-P of ATP at different time points: (A) 0 min; (B) 15 min; (C) 30 min; and (D) 120 min. The number of atoms of ^{18}O in each of the peaks of a doublet of the γ-phosphorus group is noted. Details are described in Expermental Procedures.

human ACL. From the present studies as well as the steady-state kinetic mechanism (Scheme 2), a mechanistic model of the biosynthetic reaction catalyzed by ACL reaction can be built. With the mechanism in Scheme 2, however, the rate constants describing interconversion species (E-P-cit ↔ E-citryl-P; E-citryl-P-CoA ↔ E-P-citryl-CoA) cannot be defined from the steady-state kinetic data. There is also insufficient data to define the rates of desorption of oxaloacetate and acetyl-CoA in separate steps. The ACL-catalyzed reaction is therefore simplified (Scheme 4) for evaluation of relevant microscopic rate constants. In Scheme 4, the binding and activation of citrate (also for the case of CoA) are combined into a single step. In addition, the retro-Claisen reaction is depicted to occur following phosphate release and is combined into the final product release step (k_{13}). The experimental values of kinetic parameters are expressed as functions of microscopic rate constants, in accordance with the mechanism shown in Scheme 4. These kinetic parameters for the biosynthetic reaction of ACL include the experimental values of k_{cat} (2.4 ± 0.9 s^{-1}), k_{cat}/K_m for ATP (0.019 μM^{-1} s^{-1}), k_{cat}/K_m for citrate (0.24 μM^{-1} s^{-1}), k_{cat}/K_m for CoA (0.24 μM^{-1} s^{-1}), as defined by eqs 8−11. The net rate constants $k_{x'}$[35] in k_{cat} equations are further defined by eqs 8a−8g for the biosynthetic reaction among which A, B, and C, are the concentrations of ATP, citrate, and CoA, respectively. Using the method of net rate constants,[35] eq 12 defines an expression for the steady-state levels of phosphorylated forms of ACL (E-[^{33}P]-MgADP + E-[^{33}P]-citrate + E-[^{33}P]-citryl-CoA) divided by the concentration of total enzyme forms. From the pre-steady-state kinetics, expressions for the biosynthetic reaction may be derived from the mechanism in Scheme 4 (where we assume that k_3 and $k_4 > k_5$) for the burst amplitude (eqs 13−15) and the transient rate (eqs 16−19), for which eqs 13 and 16 have the same forms as eq 4 and 3, respectively, which were used to fit the data in Figure 3. From the limiting values of the transient rate and burst amplitude obtained by the fitted replots found in Figure 3B,C and from eqs 14, 15, and 17, we obtained: λ_{max} = 63 ± 9 s^{-1}; β/E_{tmax} = 0.39 ± 0.02; and K_{d3} = 120 ± 23 μM, from which k_3 = 25 ± 5 s^{-1} and $k_4 + k_5$ = 38 ± 18 s^{-1} can be calculated.

$$k_{cat} = \frac{1}{\frac{1}{k_1'} + \frac{1}{k_3'} + \frac{1}{k_5'} + \frac{1}{k_7'} + \frac{1}{k_9'} + \frac{1}{k_{11}'} + \frac{1}{k_{13}'}} \quad (8)$$

$$k_1' = \frac{k_1 k_3 k_5 A}{k_2 k_4 + k_2 k_5 + k_3 k_5} \quad (8a)$$

$$k_3' = \frac{k_3 k_5}{k_4 + k_5} \quad (8b)$$

$$k_5' = k_5 \quad (8c)$$

dx.doi.org/10.1021/bi300611s | *Biochemistry* 2012, 51, 5198−5211

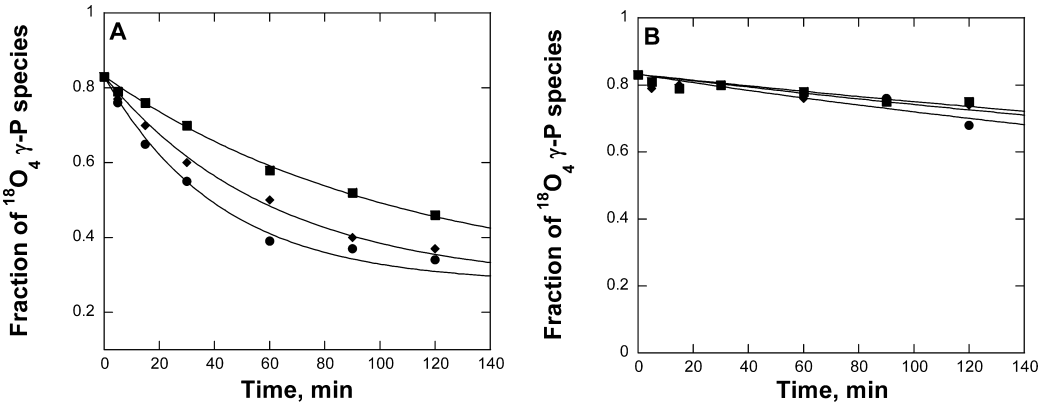

Figure 6. The fractional decrease of the [γ-$^{18}O_4$]-P species as a function of time, for wild type (A) and H760A mutant (B) ACL. Experiments were carried out with MgATP only (●), with MgATP and citrate (■), and with all three substrates (♦). The curves are fits to eq 7. Details are described in Experimental Procedures.

Table 4. Summary of ACL PIX Data[a]

	wild type		H760A	
reaction	v_{ex}, min^{-1}[b]	k_{pix}, s^{-1}[c]	v_{ex}, min^{-1}[b]	k_{pix}, s^{-1}[c]
E + MgATP	0.024 ± 0.001	14 ± 1	0.0023 ± 0.0003	0.09 ± 0.01
E + MgATP + citrate	0.009 ± 0.001	5 ± 1	0.0018 ± 0.0002	0.07 ± 0.01
E + MgATP + citrate + CoA	0.016 ± 0.001	10 ± 1	0.0018 ± 0.0003	0.07 ± 0.01

[a]Experiments were carried out with 3 mM [γ-$^{18}O_4$]-ATP, as described in Experimental Procedures. [b]Data were obtained by fitting ^{31}P NMR data to eq 7. [c]k_{pix} values were calculated using the concentrations of active sites of 84 nM and 5.12 μM for wild type and H760A ACL, respectively, assuming all four active sites are equally active.

Scheme 4

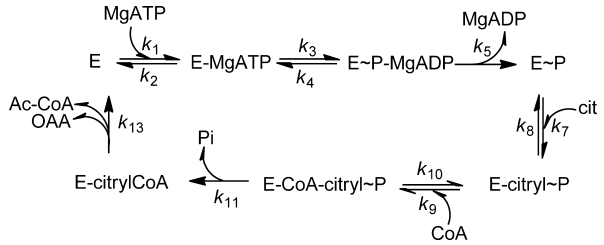

Scheme 5

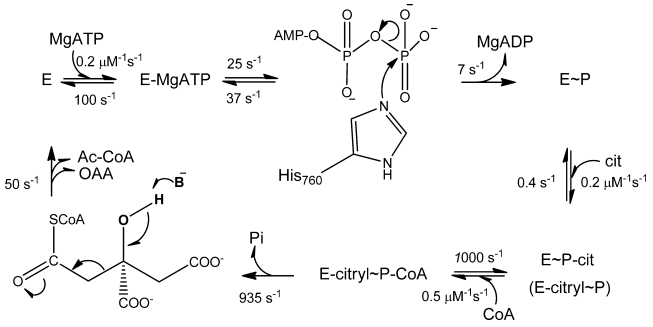

$$k_7' = \frac{k_7 k_9 k_{11} BC}{k_8 k_{10} + k_8 k_{11} + k_9 k_{11} C} \quad (8d)$$

$$k_9' = \frac{k_9 k_{11} C}{k_{10} + k_{11}} \quad (8e)$$

$$k_{11}' = k_{11} \quad (8f)$$

$$k_{13}' = k_{13} \quad (8g)$$

$$\frac{k_{cat}}{K_{ATP}} = \frac{k_1 k_3 k_5}{k_2 k_4 + k_2 k_5 + k_3 k_5} \quad (9)$$

$$\frac{k_{cat}}{K_{cit}} = \frac{k_7 k_9 k_{11} C}{k_8 k_{10} + k_8 k_{11} + k_9 k_{11} C} \quad (10)$$

$$\frac{k_{cat}}{K_{CoA}} = \frac{k_9 k_{11}}{k_{10} + k_{11}} \quad (11)$$

$$\frac{E_{pix\text{-}qua}}{E_t} = \frac{\frac{1}{k_3'} + \frac{1}{k_5'} + \frac{1}{k_7'} + \frac{1}{k_9'} + \frac{1}{k_{11}'}}{\frac{1}{k_1'} + \frac{1}{k_3'} + \frac{1}{k_5'} + \frac{1}{k_7'} + \frac{1}{k_9'} + \frac{1}{k_{11}'} + \frac{1}{k_{13}'}} \quad (12)$$

$$\frac{\beta}{E_t} = \frac{\beta_{max} A}{E_t (A + K_{d3})} \quad (13)$$

$$K_{d3} = \frac{k_2 k_4}{k_1 (k_3 + k_4 + k_5)} \quad (14)$$

$$\frac{\beta_{max}}{E_t} = \frac{k_3}{k_3 + k_4 + k_5} \quad (15)$$

$$\lambda = \frac{\lambda_{qua\text{-}max} A + K_{d2}}{A + K_{d1}} \quad (16)$$

$$\lambda_{max\text{-}qua} = k_3 + k_4 + k_5 \quad (17)$$

$$K_{d1} = \frac{k_2}{k_1} \quad (18)$$

dx.doi.org/10.1021/bi300611s | Biochemistry 2012, 51, 5198−5211

$$K_{d2} = \frac{k_2 k_4}{k_1} \quad (19)$$

$$k_{pix\text{-}bi} = \frac{k_4'}{k_5''\left(\frac{1}{k_{1'}} + \frac{1}{k_{3'}} + \frac{1}{k_{5''}}\right)} \quad (20)$$

$$k_4' = \frac{k_2 k_4}{k_2 + k_3} \quad (21)$$

$$k_{pix\text{-}ter} = \frac{k_4'}{k_5''\left(\frac{1}{k_{1'}} + \frac{1}{k_{3'}} + \frac{1}{k_{5''}} + \frac{1}{Bk_7}\right)} \quad (22)$$

$$k_{pix\text{-}qua} = k_4'\left(\frac{\frac{1}{k_5'}}{\frac{1}{k_1'} + \frac{1}{k_3'} + \frac{1}{k_5'} + \frac{1}{k_7'} + \frac{1}{k_9'} + \frac{1}{k_{11}'} + \frac{1}{k_{13}'}}\right) \quad (23)$$

Another set of relationships comes from the PIX studies. The maximal rate of positional isotope exchange for wild type ACL under binary reaction conditions (in the absence of citrate and CoA), $k_{pix\text{-}bi}$ = 14 s^{-1}, can be expressed as eq 20, for which the net rate constant of k_4' is further defined as eq 21 for the binary, ternary, and quaternary reactions. The rate of desorption of MgADP (k_5'') from the ACL-phospho-MgADP and ACL-phospho-MgADP-citrate complexes for the respective binary and ternary reactions is assumed to be near zero, due to the finding that while ACL may be quantitatively phosphorylated under these reaction conditions in an apparent single turnover event, the observance of PIX demonstrates that MgATP may be re-formed from the "moribund" phospho-enzyme-MgADP complex. The observed rates of PIX for ternary and quaternary reaction conditions are expressed as shown below in eqs 22 and 23, respectively.

Simultaneous solutions for the 11 experimental kinetic parameters for the biosynthetic reaction of ACL as defined by eqs 8−19, and 23 were attempted using the NLIN procedure available in SAS software (SAS 9.1.3 on a Service Pack 2 on a XP Pro Platform; Cary, North Carolina, USA), which employs a Levenberg−Marquardt algorithm to produce least-squares or weighted least-squares estimates of the variables. In addition, we fixed k_3 to the experimentally determined value of 25 ± 5 s^{-1}. This provided at least one set of self-consistent, "candidate" values for the individual rate constants shown in Table 5. It is important to note that these values do not represent the absolute rates for the steps and are therefore referred as "candidate" values. When these candidate rate constants were inserted into eqs 8−19 and 23, the resulting calculated kinetic parameters were, as expected, in good agreement with their corresponding experimental values (Table 6). This calculated model indicated that the release of MgADP (k_5 = 7 s^{-1}) is the rate-limiting step for the biosynthetic reaction of ACL catalysis and that the formation of the phospho-enzyme-MgADP complex is relatively slow and readily reversible (k_3/k_4 = 0.7). In addition, the collapse of the citryl-AcCoA intermediate via the retro-Claisen reaction and subsequent release of the final products (k_{13} = 50 s^{-1}) occurred at a rate similar to that of formation of phospho-ACL (k_3 = 25 s^{-1}).

We next employed KinTek Explorer to simulate the experimental time courses of the pre-steady-state formation of [^{33}P]-ACL in the binary and ternary reactions (Figure 2), and for the biosynthetic reaction at variable concentrations of MgATP (Figure 3A), using the calculated individual rate constants in Table 5. The simulated time courses generated are shown in Figures 7A,B, and as expected, are in good agreement with the experimental time courses of Figures 2 and 3A.

Table 5. Candidate Values for Rate Constants Obtained by Simulation and Calculation[a]

rate constant	value	unit
k_1	0.2	$\mu M^{-1}\ s^{-1}$
k_2	100	s^{-1}
k_3	25	s^{-1}
k_4	37	s^{-1}
k_5	7	s^{-1}
$k_{5''}$	0.008	s^{-1}
k_7	0.2	$\mu M^{-1}\ s^{-1}$
k_8	0.4	s^{-1}
k_9[b]	0.5	$\mu M^{-1}\ s^{-1}$
k_{10}[b]	1000	s^{-1}
k_{11}	935	s^{-1}
k_{13}	50	s^{-1}

[a]Experiments were carried out using SAS statistical programming, as well as calculation described in Experimental Procedures. The value of k_3 was fixed as the experimentally determined value of 25 ± 5 s^{-1}. [b]Values could not be determined by SAS, nor simulation, details in Results.

Table 6. Experimental and Calculated Kinetic Parameters for ACL[a]

equation number	kinetic parameter	experimental values	calculated values	units
8	k_{cat}	2.4 ± 0.9	2.4	s^{-1}
9	k_{cat}/K_{MgATP}	0.019 ± 0.007	0.01	$\mu M^{-1}\ s^{-1}$
10	$k_{cat}/K_{citrate}$	0.23 ± 0.07	0.20	$\mu M^{-1}\ s^{-1}$
11	k_{cat}/K_{CoA}	0.24 ± 0.11	0.24	$\mu M^{-1}\ s^{-1}$
12	$E_{pix\text{-}qua}/E_t$	0.34 ± 0.02	0.39	N.A.
15	$\beta_{qua\text{-}max}/E_t$	0.39 ± 0.02	0.36	N.A.
17	$\lambda_{qua\text{-}max}$	63 ± 9	69	s^{-1}
18	K_{d1}	500 ± 200	500	μM
20	$k_{pix\text{-}bi}$	14 ± 7	11	s^{-1}
22	$k_{pix\text{-}ter}$	5 ± 1	6	s^{-1}
23	$k_{pix\text{-}qua}$	10 ± 3	9	s^{-1}

[a]Experimental kinetic parameters are those found in this work and reported in Tables 1−4. Calculated kinetic parameters were obtained from simultaneous solution of the 11 equations in column 1 using the candidate individual rate constants in Table 5. The calculated kinetic parameters in column 4 were then obtained by insertion of the candidate individual rate constants into the equations found in column 1. The calculated kinetic parameters agree with experimental results within experimental error of these values.

DISCUSSION

The Essential Role of His760. His760 is necessary for the biosynthetic reaction of ACL. The catalytic role of an active site histidine was implicated by the DEPC-mediated inactivation of wild type ACL, which was abrogated in the presence of MgATP. The recovery of enzymatic activity by the addition of hydroxylamine to DEPC-inactivated ACL is indicative of the deacylation of an *N*-carboethoxy-histidine, as opposed to more stable N-carboethoxy enzymatic residues.

dx.doi.org/10.1021/bi300611s | *Biochemistry* 2012, 51, 5198−5211

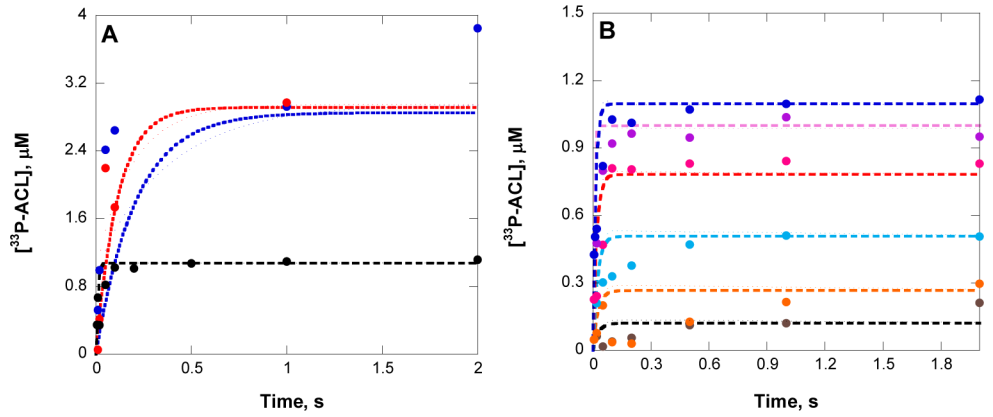

Figure 7. Simulation results as obtained using KinTek Global Kinetic Explorer. The simulated data are represented as dotted traces. The time courses were obtained from the candidate rate constants found in Table 6. The experimentally measured data are shown in solid dots. (A) Simulation of single-turnover time courses for ACL and 0.5 mM citrate at 1.5 mM [γ-^{33}P]-MgATP in the absence of citrate and CoA (black), in the presence of 0.5 mM citrate (blue), and in the presence of 0.5 mM CoA and citrate (black). (B) Simulation of single-turnover time courses for ACL in the presence of 0.5 mM citrate and CoA, using variable concentrations of [γ-^{33}P]-MgATP, at 15.36 (gray), 38.4 (orange), 96 (red), 240 (magenta), 600 (purple), and 1500 (blue) μM.

His760 serves as the catalytic phosphate acceptor to initiate the biosynthetic reaction of ACL. Evidence comes from the production of stable, isolable phosphorylated forms of wild type ACL as probed by the use of [^{33}P]-MgATP and by the pH-dependence of pre-steady-state kinetic studies with wild type ACL (Figure 4). A pK_a value of 7.5 of an essential, unprotonated enzymatic residue was critical to phosphorylation of ACL, and this finding is in excellent agreement with the identity of this residue as an unprotonated histidine. In addition, the catalytic importance of His760 in phosphorylation is further indicated by two other observations: (1) the inactivation of ACL by DEPC can be fully blocked by adding ATP (Figure 1); and (2) H760A is unable to catalyze the formation of the final biosynthetic product, oxaloacetate.

ACL belongs to the acyl-CoA synthase (nucleoside diphosphate, NDP-forming) superfamily.[36] A recent breakthrough in the structural characterization of ACL has been achieved.[37] However, a structural motif containing the putative active site His760 was not observed in the published structure, presumably as a result of the proteolytic conditions used to obtain a diffracting crystal.[37] The structure of ACL reveals a similar tertiary fold to succinyl-CoA synthetase (SCS), especially in the vicinity of the ATP binding site.[37] SCS catalyzes the reversible formation of succinyl-CoA from succinate and CoA using either GTP or ATP as the source of activated phosphate.[38−40] The active site histidinyl residue is strictly conserved between ACL and SCS by sequence alignment. In the structure of *Escherichia coli* SCS, the catalytic His246 was clearly observed to show phosphorylation of the Nε2 atom of His246.[41]

There might be a second residue in ACL that serves as a phosphate acceptor. Data supporting this hypothesis arise from both the steady-state production of phosphate and MgADP from the wild type and H760A mutant of ACL in the absence of citrate and CoA (using the phosphate sensor and ADP-Glo assays), as well as the positional isotope exchange observed with H760A ACL. The rates of such "unproductive phosphorylation" are less than 1% of the k_{cat} for the full biosynthetic reaction. The candidacy of the second phosphorylation site is unclear at this point.

Reversible Phosphate Intermediates. The phosphoenzyme intermediates, that is, E−Pi-MgADP, E-Pi-citrate, and E−Pi-citrate-CoA are formed during ACL catalysis, and are highly reversible. Direct evidence comes from the PIX studies. PIX studies were initially used to address whether the phosphate transfer occurs through a phospho-enzyme intermediate or by a direct in-line attack. PIX has been used to understand the nature of enzyme-bound intermediates in NDP- or NMP-forming enzymes including glutamate synthetase,[42] carbamoyl phosphate synthetase,[43] and *Mycobacterium smegmatis* cysteine lyase, MshC.[44] These enzymes utilize transfer of the γ-phosphate ATP (or β-pyrophosphate for MshC) to activate substrate in these reactions, in similar fashion to that of ACL. A high rate of positional isotope exchange of (14 s^{-1}) was observed when MgATP is incubated as the only substrate with ACL. This exchange rate is the largest PIX rate reported thus far.[45] The rapid exchange rate is also consistent with MgADP release being at least partially rate-limiting in the biosynthetic reaction.

The observed double-displacement mechanism of ACL rules out the direct transfer of phosphate from ATP to citrate and is in excellent agreement with the Ping Pong kinetic mechanism observed between ATP and citrate as shown in Scheme 2.[5,11−13] For enzymes that strictly utilize direct phosphoryl-transfer from ATP to the cosubstrate, for example, carbamoyl phosphate synthetase[46] and glutamine synthetase,[42] no isotope exchange was observed unless a second substrate was present. The free scrambling of ^{18}O at the β-P position gives a ~33% chance of ^{16}O to reside at the β, γ-bridging position. In fact, only 39% [γ-$^{18}O_4$]-ATP remained after 1 h of incubation with ACL, indicating that in the binary reaction of wild type ACL that positional isotope exchange was virtually completed (Figure 6).

Addition of citrate to a reaction mixture containing [γ-$^{18}O_4$]-ATP and wild type ACL resulted in a decrease of the PIX rate, due to the reduced dissociation of MgATP exchanged from the enzyme upon the introduction of citrate. This agrees well with the proposed ordered binding of ATP and citrate. If citrate were to bind prior to MgATP, or to have a random order of binding with regard to MgATP, then no decrease in the PIX rate would be expected as was the case reported for MshC.[44] Inspection of the expressions for k_{pix} under binary (eq 21, $k_{pix\text{-}bi}$ = 14 s^{-1}) and ternary (eq 23, $k_{pix\text{-}ter}$ = 5 s^{-1}) reveals that a small value of k_7'', representing the binding of citrate, and possibly its

dx.doi.org/10.1021/bi300611s | *Biochemistry* 2012, 51, 5198−5211

progressing to the dead-end E-citryl-P complex, could render $k_{pix\text{-}ter} < k_{pix\text{-}bi}$. The reversibility of PIX under ternary reaction conditions is also in accord with the formation of an ACL-citryl-phosphate intermediate, and not a covalent citryl-ACL adduct.[16,47] Under this condition, the decreased, yet significant, value of the PIX rate observed in the presence of citrate primarily arises from reversal of the initial phosphoryl-transfer reaction as characterized by k_4'. Reconciliation of this interpretation requires that k_5 contributes to rate limitation of all three reaction conditions (vide infra).

It should also be noted that adding CoA did not further decrease the PIX rate. That the desorption of MgADP from the E−P-MgADP complex is overall rate-limiting to the biosynthetic reaction, and that the inclusion of CoA reduces this complex from ≤100% to 34% of total enzyme forms, also gives rise to reduction of the rate of PIX to 10 s^{-1}. Under full biosynthetic reaction conditions, $k_{pix\text{-}qua}$ exceeds $k_{pix\text{-}ter}$ because free enzyme is regenerated from additional rounds of PIX, and the enzyme is not "locked" into the dead end E-citryl-P complex of the ternary reaction.

An unknown phosphate acceptor of ACL would still be able to regenerate exchanged ATP. The PIX rate for H760A is significantly decreased compared to that of wild type ACL, that is, ∼150 fold less. The PIX rates for H760A ACL were found to be virtually unchanged upon the addition of citrate and/or CoA, which is not surprising, as the mutant enzyme cannot proceed with reaction beyond the phosphorylation reactions.

Possible Rate-Limiting Step(s). Modeling of our kinetic data is consistent with the presence of three steps that likely contribute to rate limitation of ACL catalysis under saturating concentrations of all three substrates. These steps include k_3 (25 s^{-1}), k_5 (7 s^{-1}), and k_{13} (50 s^{-1}) in Scheme 4, such that k_5 is the slowest step in ACL turnover. Accordingly, the release of the first product, MgADP, is the primary determinant of the overall turnover number of human ACL.

The release of MgADP being a slow step in catalysis is supported by the observation of a rapid PIX rate observed in wild type ACL. The slow release of MgADP allows the reformation of MgATP from the E−P-MgADP intermediate. The notion that k_5 is a slow step can readily explain the finding that the PIX rate is suppressed by adding citrate. The burst observed in rapid kinetics is therefore largely composed of E−P-MgADP instead of E−P.

The contribution to rate-limitation of the k_{13} step likely arises from the retro-Claisen reaction of the citryl-CoA. In the mechanism proposed in Scheme 4, k_{13} comprises the release(s) of final products as well as the chemical step. The cleavage of citryl-CoA is proposed to proceed via a general base catalysis.[11] However, the contribution to rate from the release of oxaloacetate and acetyl CoA cannot be completely ruled out.[a]

The binding energy values provide additional insights for the assignment of rate-limiting step(s) from a different perspective. It is important to note that values from binding energies can only provide information regarding the rate-limiting nature of either substrate binding or product release, but not the intermediary catalytic steps. The binding energy can be calculated using eq 24,[48] in which R is the gas constant, and T is temperature in Kelvin. For citrate and CoA, the dissociation constants (K_{ib}, K_{ic}) were used in place of K_d; for inorganic phosphate, MgADP, oxaloacetate, and acetyl-CoA, the inhibition constant values (K_i) were used in place of K_d. The values obtained describe energy expense in terms of "binding" events; hence for the events of "product release", the signs of calculated energy were reversed. Figure 8 shows the binding/release energy profile constructed using these values

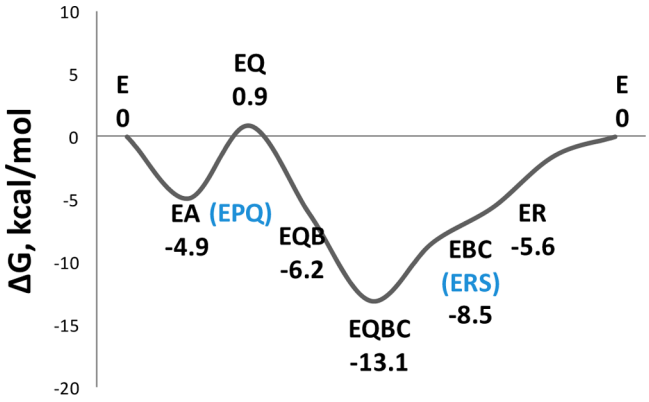

Figure 8. Binding and dissociation energy profile for substrates and products in the biosynthetic reaction catalyzed by ACL. The ΔG values in units of kcal/mol are listed in numbers. The steps involved in catalysis are shown in blue. Here A, B, and C represent substrates: MgATP, citrate and CoA, respectively; P, Q, R, and S represent product: ADP, inorganic phosphate, acetylCoA, and oxaloacetate, respectively.

for the ACL biosynthetic reaction. Free enzyme was used as a "reference" free energy, and assigned a value of zero. It is interesting that in this diagram, the step from E-MgADP−P to E−P is on the highest free energy point among all the reactant/intermediate states; indeed it shows that the release of MgADP is an "energy-expensive" step for ACL, supporting the notion that MgADP release is slow.

$$\Delta G_{binding} = RT \ln(K_d) \quad (24)$$

Enzymes that catalyze related reactions using A(G)TP activation of substrates are of broad interests in mechanistic, biochemical, and biomedical aspects. For those enzymes, the identity of the rate-limiting step(s) remains a key question. The rate of the biosynthetic reaction by glutamate synthetase is limited by release of MgADP.[42] For the two classes of aminoacyl-tRNA synthetases, the rate-limiting step in class I enzymes has been suggested to be the release of aminoacyl-tRNA,[49] and class II enzymes employ chemistry step(s), that is, adenylation or a combination with the subsquent aminoacyl transfer, to determine the rate of turnover.[49−51] The rate-limiting step of 5-aminolevulinate synthetase, another NDP-forming acyl-CoA synthetase enzyme, was determined to be the release of 5-aminolevulinate.[52] The reactions from all above enzymes can be viewed as "partial ACL reactions" in that they proceed via both ATPase and ligation steps (first two partial reactions), while lacking the subsequent retro-Claisen reaction. Hence the assignment of rate-limiting step(s) in ACL represents the first-in-class study for an enzyme that catalyze ligase-then-cleavage reactions using A(G)TP-catalyzed activation.

SUMMARY

ATP citrate lyase (ACL) catalyzes the ATP-dependent biosynthesis of acetyl-Coenzyme A and oxaloacetate from citrate and coenzyme A (CoA). Although the enzyme is of broad interest and has been studied for decades, its chemical mechanism remains undefined. We have carried out detailed mechanistic characterization in order to address three key

questions: the role of the active site histidine; the nature of the phosphorylated intermediates formed in the reaction path; and the possible rate contributing step(s) in the biosynthetic reaction. Chemical modification, steady-state and pre-steady-state kinetics, and the pH-dependent rapid kinetics have collectively demonstrated the essential role of the active site His760 in ACL reaction. His760 acts as a phosphate acceptor to initiate the biosynthetic reaction. There is also a second phosphate acceptor in the ACL active site. The phosphorylation of this residue occurs at a rate that is 3 orders of magnitude lower than that of the wild type enzyme and produces no acetyl-CoA and oxaloacetate. The high PIX rates for the binary, ternary, and quaternary reaction of ACL indicates that the ACL-phospho-histidinyl intermediate is highly reversible under all reaction conditions, owing in part to the rate-limiting desorption of MgADP. The β,γ-bridge to nonbridge positional isotope exchange rate of [γ-$^{18}O_4$]-ATP achieved its maximal rate of 14 s^{-1} in the absence of citrate and CoA, the highest PIX rate reported thus far. Computational studies have determined that the k_5 step occurs at a rate of ~7 s^{-1}, thus is the slowest step in the biosynthetic reaction. Targeting these possible steps is therefore an efficient strategy for rational inhibitor design.

AUTHOR INFORMATION

Corresponding Author

*Tel: 610.917.6238. Fax: 610.917.7379. E-mail: fan.x.fan@gsk.com.

Notes

The authors declare no competing financial interest.

ACKNOWLEDGMENTS

The authors thank Dr. Jennifer L. Ariazi (GlaxoSmithKline) for her generous support in carrying out mechanistic studies on ACL. The authors also thank Martin Brandt and Amber D. Jones (GlaxoSmithKline) for their initiation of ACL assay development, as well as thorough steady-state kinetic studies. The authors owe much appreciation to Dr. Andrew S. Murkin (Department of Chemistry, University of Buffalo, the State University of New York) for his crucial contribution of suggesting the pH-dependent rapid kinetic studies, and to Clarissa Melo Czekster (Department of Biochemistry, Albert Einstein College of Medicine) for her valuable suggestions on KinTek simulation of the microscopic rate constants.

ABBREVIATIONS USED

ACL: ATP citrate lyase; CoA: coenzyme A; SDS−PAGE: sodium dodecyl sulfate polyacrylamide gel electrophoresis; DTT: dithiothreitol; EDTA: ethylenediaminetetraacetic acid; MOPS: 3-(*N*-morpholino)propanesulfonic acid; Tris: tris-(hydroxymethyl)aminomethane; DEPC: diethylpyrocarbonate; SCS: succinyl-CoA synthetase; PIX: positional isotope exchange; SAS: statistical analysis system

ADDITIONAL NOTE

[a]It is important to note that the contribution from each one of the three steps in k_{13} (retro-Claisen cleavage of citryl CoA, as well as the releases of oxaloacetate and acetyl-CoA) to the overall turnover of ACL is not significant, as the value of each individual step is larger than 20 times k_{cat}.

REFERENCES

(1) Inoue, H., Suzuki, F., Tanioka, H., and Takeda, Y. (1967) Role of ATP in the ATP citrate lyase reaction. *Biochem. Biophys. Res. Commun. 26*, 602−608.

(2) Inoue, H., Suzuki, F., Tanioka, H., and Takeda, Y. (1968) Studies on ATP citrate lyase of rat liver. 3. The reaction mechanism. *J. Biochem. 63*, 89−100.

(3) Inoue, H., Tsunemi, T., Suzuki, F., and Takeda, Y. (1969) Studies on ATP citrate lyase of rat liver. IV. The role of CoA. *J. Biochem. 65*, 889−900.

(4) Linn, T. C., and Srere, P. A. (1979) Identification of ATP citrate lyase as a phosphoprotein. *J. Biol. Chem. 254*, 1691−1698.

(5) Plowman, D. M., and Cleland, W. W. (1967) Purification and kinetic studies of the citrate cleavage enzyme. *J. Biol. Chem. 242*, 4239−4247.

(6) Spencer, A. F., and Lowenstein, J. M. (1966) Citrate and the conversion of carbohydrate into fat. Citrate cleavage in obesity and lactation. *Biochem. J. 99*, 760−765.

(7) Takeda, Y., and Inoue, H. (1968) [ATP citrate lyase]. *Tanpakushitsu Kakusan Koso 13*, 720−729.

(8) Des Rosiers, C., Di Donato, L., Comte, B., Laplante, A., Marcoux, C., David, F., Fernandez, C. A., and Brunengraber, H. (1995) Isotopomer analysis of citric acid cycle and gluconeogenesis in rat liver. Reversibility of isocitrate dehydrogenase and involvement of ATP-citrate lyase in gluconeogenesis. *J. Biol. Chem. 270*, 10027−10036.

(9) Sullivan, A. C., Triscari, J., and Halmilton, J. G. (1973) Effect of (−)-hydroxycitrate upon the accumulation of lipid in the rat: I. Lipogenesis. *Lipids 9*, 121−128.

(10) Wellen, K. E., Hatzivassiliou, G., Sachdeva, U. M., Bui, T. V., Cross, J. R., and Thompson, C. B. (2009) ATP-citrate lyase links cellular metabolism to histone acetylation. *Science 324*, 1076−1080.

(11) Rokita, S. E., Srere, P. A., and Walsh, C. T. (1982) 3-Fluoro-3-deoxycitrate: a probe for mechanistic study of citrate-utilizing enzymes. *Biochemistry 21*, 3765−3774.

(12) Srere, P. A. (1975) The enzymology of the formation and the breakdown of citrate. *Adv. Enzymol. Relat. Areas. Mol. Biol. 43*, 57−101.

(13) Walsh, C. T., Jr., and Spector, L. B. (1969) Citryl phosphate and the mode of action of the citrate cleavage enzyme. *J. Biol. Chem. 244*, 4366−4374.

(14) Houston, B., and Nimmo, H. G. (1984) Purification and some kinetic properties of rat liver ATP citrate lyase. *Biochem. J. 224*, 437−443.

(15) Patel, M. S., and Owen, O. E. (1976) Lipogenesis from ketone bodies in rat brain. Evidence for conversion of acetoacetate into acetyl-coenzyme A in the cytosol. *Biochem. J. 156*, 603−607.

(16) Wells, T. N. (1991) ATP-citrate lyase from rat liver. Characterisation of the citryl-enzyme complexes. *Eur. J. Biochem. 199*, 163−168.

(17) Williams, S. P., Sykes, B. D., and Bridger, W. A. (1985) Phosphorus-31 nuclear magnetic resonance study of the active site phosphohistidine and regulatory phosphoserine residues of rat liver ATP-citrate lyase. *Biochemistry 24*, 5527−5531.

(18) Krivanek, J., and Novakova, L. (1991) ATP-citrate lyase is another enzyme the histidine phosphorylation of which is inhibited by vanadate. *FEBS Lett. 282*, 32−34.

(19) Kanao, T., Fukui, T., Atomi, H., and Imanaka, T. (2002) Kinetic and biochemical analyses on the reaction mechanism of a bacterial ATP-citrate lyase. *Eur. J. Biochem. 269*, 3409−3416.

(20) Besant, P. G., and Attwood, P. V. (2009) Detection and analysis of protein histidine phosphorylation. *Mol. Cell. Biochem. 329*, 93−106.

(21) Puttick, J., Baker, E. N., and Delbaere, L. T. (2008) Histidine phosphorylation in biological systems. *Biochim. Biophys. Acta 1784*, 100−105.

(22) Berwick, D. C., Hers, I., Heesom, K. J., Moule, S. K., and Tavare, J. M. (2002) The identification of ATP-citrate lyase as a protein kinase B (Akt) substrate in primary adipocytes. *J. Biol. Chem. 277*, 33895−33900.

(23) Potapova, I. A., El-Maghrabi, M. R., Doronin, S. V., and Benjamin, W. B. (2000) Phosphorylation of recombinant human

ATP:citrate lyase by cAMP-dependent protein kinase abolishes homotropic allosteric regulation of the enzyme by citrate and increases the enzyme activity. Allosteric activation of ATP:citrate lyase by phosphorylated sugars. *Biochemistry 39*, 1169−1179.
(24) Ramakrishna, S., D'Angelo, G., and Benjamin, W. B. (1990) Sequence of sites on ATP-citrate lyase and phosphatase inhibitor 2 phosphorylated by multifunctional protein kinase (a glycogen synthase kinase 3 like kinase). *Biochemistry 29*, 7617−7624.
(25) Wagner, P. D., and Vu, N. D. (1995) Phosphorylation of ATP-citrate lyase by nucleoside diphosphate kinase. *J. Biol. Chem. 270*, 21758−21764.
(26) Ugochukwu, E., Shafqat, N., Rojkova, A., Sundstrom, M., Arrowsmith, C., Weigelt, J., Edwards, A., Von Delft, F., Oppermann, U. (2006) MDH2: Human malate dehydrogenase type 2, Structural Genomics Consortium (SGC).
(27) Schneck, J. L., Briand, J., Chen, S., Lehr, R., McDevitt, P., Zhao, B., Smallwood, A., Concha, N., Oza, K., Kirkpatrick, R., Yan, K., Villa, J. P., Meek, T. D., Thrall, S. H. Kinetic mechanism and rate-limiting steps of focal adhesion kinase-1, *Biochemistry 49*, 7151−7163.
(28) Lord, K. A., Wang, X. M., Simmons, S. J., Bruckner, R. C., Loscig, J., O'Connor, B., Bentley, R., Smallwood, A., Chadwick, C. C., Stevis, P. E., and Ciccarelli, R. B. (1997) Variant cDNA sequences of human ATP:citrate lyase: cloning, expression, and purification from baculovirus-infected insect cells. *Protein Expr. Purif. 9*, 133−141.
(29) Laemmli, U. K. (1970) Cleavage of structural proteins during the assembly of the head of bacteriophage T4. *Nature 227*, 680−685.
(30) Bradford, M. M. (1976) A rapid and sensitive method for the quantitation of microgram quantities of protein utilizing the principle of protein-dye binding. *Anal. Biochem. 72*, 248−254.
(31) Midelfort, C. F., and Rose, I. A. (1976) A stereochemical method for detection of ATP terminal phosphate transfer in enzymatic reactions. Glutamine synthetase. *J. Biol. Chem. 251*, 5881−5887.
(32) Lundblad, R. L. (2004) *Chemical Reagents for Protein Modification*, 3rd ed., CRC Press, Boca Raton, FL.
(33) Miles, E. W. (1977) Modification of Histidyl Residues in Proteins by Diethylpyrocarbonate, in *Methods in Enzymology*, Vol. 47, pp 431−442, Elsevier, Amsterdam.
(34) This is calculated using the molar extinction coefficient of the histidinyl-DEPC adduct, that is 3200 M^{-1} cm^{-1}, also with the assumption that all histidine residues were modified.
(35) Cleland, W. W. (1975) Partition analysis and concept of net rate constants as tools in enzyme kinetics. *Biochemistry 14*, 3220−3224.
(36) Sanchez, L. B., Galperin, M. Y., and Muller, M. (2000) Acetyl-CoA synthetase from the amitochondriate eukaryote Giardia lamblia belongs to the newly recognized superfamily of acyl-CoA synthetases (Nucleoside diphosphate-forming). *J. Biol. Chem. 275*, 5794−5803.
(37) Sun, T., Hayakawa, K., Bateman, K. S., Fraser, M. E. Identification of the citrate-binding site of human ATP-citrate lyase using X-ray crystallography, *J. Biol. Chem. 285*, 27418−27428.
(38) Kaufman, S. (1953) Succinyl coenzyme A and its role in phosphorylation. *Fed. Proc. 12*, 704−708.
(39) Sanadi, D. R., Gibson, D. M., Ayengar, P., and Jacob, M. (1956) Alpha-ketoglutaric dehydrogenase. V. Guanosine diphosphate in coupled phosphorylation. *J. Biol. Chem. 218*, 505−520.
(40) Weitzman, P. D. (1981) Unity and diversity in some bacterial citric acid-cycle enzymes. *Adv. Microb. Physiol. 22*, 185−244.
(41) Fraser, M. E., James, M. N., Bridger, W. A., and Wolodko, W. T. (1999) A detailed structural description of *Escherichia coli* succinyl-CoA synthetase. *J. Mol. Biol. 285*, 1633−1653.
(42) Meek, T. D., Johnson, K. A., and Villafranca, J. J. (1982) *Escherichia coli* glutamine synthetase. Determination of rate-limiting steps by rapid-quench and isotope partitioning experiments. *Biochemistry 21*, 2158−2167.
(43) Raushel, F. M., and Villafranca, J. J. (1980) Phosphorus-31 nuclear magnetic resonance application to positional isotope exchange reactions catalyzed by *Escherichia coli* carbamoyl-phosphate synthetase: analysis of forward and reverse enzymatic reactions. *Biochemistry 19*, 3170−3174.
(44) Williams, L., Fan, F., Blanchard, J. S., and Raushel, F. M. (2008) Positional isotope exchange analysis of the Mycobacterium smegmatis cysteine ligase (MshC). *Biochemistry 47*, 4843−4850.
(45) Mullins, L. S., Raushell, F. M. (1995) Positional isotope exchange as probe of enzyme action, in *Methol. Enzymol.* (Abelson, J. N., Simmons, S. J., Eds.), pp 398−425, Academic Press, New York.
(46) Meek, T. D., Karsten, W. E., and DeBrosse, C. W. (1987) Carbamoyl-phosphate synthetase II of the mammalian CAD protein: kinetic mechanism and elucidation of reaction intermediates by positional isotope exchange. *Biochemistry 26*, 2584−2593.
(47) Marletta, M. A., Srere, P. A., and Walsh, C. (1981) Stereochemical outcome of processing of fluorinated substrates by ATP citrate lyase and malate synthase. *Biochemistry 20*, 3719−3723.
(48) Dallakyan, S. (2010) How Autodock 4 converts binding energy (kcal/mol) into Ki.
(49) Zhang, C. M., Perona, J. J., Ryu, K., Francklyn, C., and Hou, Y. M. (2006) Distinct kinetic mechanisms of the two classes of aminoacyl-tRNA synthetases. *J. Mol. Biol. 361*, 300−311.
(50) Dibbelt, L., Pachmann, U., and Zachau, H. G. (1980) Serine activation is the rate limiting step of tRNASer aminoacylation by yeast seryl tRNA synthetase. *Nucleic Acids Res. 8*, 4021−4039.
(51) Dibbelt, L., and Zachau, H. G. (1981) On the rate limiting step of yeast tRNAPhe aminoacylation. *FEBS Lett. 129*, 173−176.
(52) Hunter, G. A., and Ferreira, G. C. (1999) Pre-steady-state reaction of 5-aminolevulinate synthase. Evidence for a rate-determining product release. *J. Biol. Chem. 274*, 12222−12228.